New Nanopumping Effects with Carbon Nanotubes

Z. Insepov

Mathematics and Computer Science Division, Argonne National Laboratory,
9700 South Cass Ave., Argonne, IL 60439

ABSTRACT

Molecular dynamics (MD) simulations show macroscopic flows of atomic and molecular hydrogen, helium, and a mixture of both gases both inside and outside a carbon nanotube. In particular, the simulations show a "nanoseparation" effect of the two gases. In a previous paper we showed that propagation of Rayleigh traveling waves on the nanotube surface activates a macroscopic flow of the gas (or gases) that depends critically on the atomic mass of the gas. Our new results show the mass selectivity of the nanopumping effect can be used to develop a highly selective filter for various gases. Gas flow rates, pumping, and separation efficiencies were calculated at various wave frequencies and phase velocities of the surface waves.

INTRODUCTION

Actuation of a fluid flow in microcapillaries are of both fundamental and practical interest in the areas of nanorobotics, fine printing at the nanoscale, atom optics, quantum computing, hydrogen energetics, chemical process control, cell biology, medical drug delivery, and molecular medicine [1-10]. Microflow control is important for various industrial and commercial applications, including DNA analysis, drug screening, optical display technologies, tunable fiber optic waveguides, thermal management of semiconductor devices and lasers, clinical and forensic analysis, and environmental monitoring [1].

Most of the existing fluidic devices are based on the following physical effects: electro-osmosis, electrohydrodynamics, magnetohydrodynamics, centrifugation, pressure gradient, and modulation of the stresses at the fluid-fluid and fluid-solid interfaces [1].

Molecular dynamics (MD) simulations of some of these phenomena were reported in [2-12]. Using MD simulations, the authors of [2] showed that when the contact angle is large enough, the boundary condition can drastically differ (at a microscopic level) from a "no-slip" condition. Slipping lengths exceeding 30 molecular diameters are obtained for a contact angle of 140°, characteristic of mercury on glass. In [3,4], MD simulations were applied to polymer liquids under shear stress. At low shear rates, the shear length obtained from a Green-Kubo relation can be justified, and a general relation between the slip length and the local shear rate at a surface was obtained.

Study of fluid flows in narrow channels has become a major area of research since the discovery of nanotubes by Ijima in 1991. The microflow systems include very thin liquid films on solid surfaces [3,4], microfluid arrays [5], inhomogeneous liquid flows in narrow

slit-pores [6], in micropumps and membranes [1,7], and in three-dimensional structures with thousands of microchannels [8].

Inorganic nanotubes were successfully integrated with a microfluidic system to create the first nanofluidic device capable of sensing a single DNA molecule [9]. Various methods for atomic pumping through carbon nanotubes were proposed in [10, 11]. In [10], a laser-driven pump for atomic transport through carbon nanotube (CNT) was proposed based on the generation of electric current through the tube, which in turn would move ions in it by drag forces. A nanopipette concept for dragging metal ions through a multiwalled CNT was experimentally confirmed in [11].

Computer Simulation of Fluid Flow in Nanotubes

Computer simulation methods have been used to study microfluids [2-4,6,12-23]. Atomistic simulations of microfluid flows in nanochannels are limited.

Fluid-flow dynamics of gases and liquids in carbon nanotubes has been studied by MD in [12-16]. The movement of the walls strongly influences the helium and argon gas flows inside a carbon nanotube [12]. The effect of filling nanotubes with C_{60}, CH_4, and Ne gases on the mechanical properties of the nanotubes has been examined by MD in [13]. Interaction of fluids with microscopic pores by filling (imbibition) of nanotubes with oil or mercury is of great technological interest; indeed, the authors of [14, 15] have found that even the smallest nanotubes (7×7) imbibed at an extremely high rate ($\leq$ 800 m/s). The nanoscale imbibition does not obey a Washburn equation applicable to continuum flows. The latter predicts a square root dependence of the imbibition rate on time. However, it is a complex process showing a linear time dependence of the level of filling [14]. The authors in [15] have shown that until a threshold internal pressure is reached inside the liquid, the wetting and filling of the nanotube do not occur. The authors of ref. [16] showed that a periodic external pressure applied to liquid generates a discontinuous flow through the nanotube embedded into the liquid.

Hydrogen adsorption by graphite nanofibers and carbon nanotubes was studied by MD, grand canonical Monte Carlo, and ab initio methods in [17-20]. Liberation of atomic form of hydrogen chemisorbed on carbon materials has also been investigated. The gas-surface virial coefficient and isosteric heat of adsorption were calculated by classical methods in [17]. A review of experimental and computer simulation results of adsorption of hydrogen on carbon nanotubes and on graphitic nanofibers was given in [18].

In [19], transition metals bound to fullerenes C_{60} were found to increase hydrogen storage in carbon nanotubes. The calculated binding energy of hydrogen molecule was found to be 0.3 eV/H_2, which is an ideal value for use in vehicles. The theoretical maximum retrievable H_2 storage density is 9 wt%. This hydrogen release process is critical for future hydrogen application in the car industry. Even if the U.S. Department of Energy target of 6.5 wt% of hydrogen storage is reachable, for example, by a chemisorption mechanism, the subsequent liberation of hydrogen by heating will need very high temperatures, which makes this application unrealistic [20]. Ultrasonication of single-walled carbon nanotubes showed an uptake of hydrogen at room temperature [20]. However, the authors have assigned this uptake to possible metal contamination during the sonication process.

Rarefied Gas Flows

Contrary to the dense fluid flows in micron- and nanometer-sized channels, rarefied gas flows are of interest for future gas pumping. Microelectromechanical systems and microscale vacuum technology devices are yet another area of application [21-24]. The rarefied gas flows in a naturally occurring zeolite, clinoptilolite, for a chip-scale, thermal transpiration-based gas pump were studied in [25].

Acoustic Properties

Propagation of acoustic waves on metal cylinders and through the carbon nanotubes was discussed in [26-31]. There are a few ways to activate surface traveling waves on the nanotube surface. One way is to use short laser pulses to generate thermo-acoustic waves on a tube [30]. Another way is to send ultrasound waves through the liquid or dense gaseous media to the nanotube [31]. Rayleigh surface waves are activated when a longitudinal wave traveling in a liquid/gas impinges on a solid surface at an incidence angle equal to the Rayleigh angle θ (where θ = arcsine (C_p/C_s), C_p is the velocity of the incident wave and C_s is the velocity of the surface wave in the material [31]. Propagation of traveling waves on a dolphin skin surface was discussed in [32,33].

Research Objectives

The goal of this paper is to prove the nanopumping concept by MD simulation of a carbon nanotube device that will enable pumping gases or liquids at the nanoscale, through nanometer channels. A simple MD simulation model of gas-nanotube interaction was

developed in which the nanotube walls move in accordance with the Rayleigh surface traveling wave. This model is used to simulate the macroscopic flow of a few gases lighter than carbon (hydrogen, helium) inside the carbon nanotubes activated with the surface waves. The atomic flow rate and average velocity of the gas flow through the nanotube were calculated to verify the overall concept and the efficiency of the nanopumping. Preliminary results of nanopumping effect were published in [34].

COMPUTATIONAL MODEL

As input for the MD simulations, coordinates of the zigzag nanotube carbon atoms were generated. Tersoff [35] and Brenner [36] interaction potentials were employed to describe the carbon-carbon interactions. Various gases interacting by means of Lennard-Jones potentials with the parameters given in Table 1 were placed inside the nanotube. The system was brought into equilibrium at room temperature, and the Rayleigh transverse surface waves with phase velocity of about 22 km/s were generated by sending the traveling waves with $f = 10^6$–10^{13} Hz along the nanotube. The carbon displacements were perpendicular to the axial direction of wave propagation (so the nanotube vibrations occurred in radial directions). Radial amplitudes of the waves were chosen to be in the interval of 1–5% of the nanotube radii.

We placed 128 or 256 gas atoms with four different masses (lighter than carbon) inside the nanotube and applied a traveling wave along the nanotube surface. The interaction between the gas atoms and the nanotube and their mass was chosen such that the gas did not penetrate through the nanotube walls, even at high velocities. The following chirality numbers of the nanotubes were tested: (5×0), (15×0), (10×0), and (15×15). The total length of the nanotubes was equal to 100 Å, and their diameters were 10–20 Å. Depending on the total number of gas atoms inside the nanotube, the real simulation time was about 35 ps.

The gas-separation MD simulation model contained 128 or 256 atoms that were placed inside (or outside) the (15×0) carbon nanotube build of 1,410 carbon atoms, and the Rayleigh (traveling) surface waves were generated on the surface of the nanotubes at various frequencies, amplitudes, and phase velocities. When the gases were placed outside the nanotube, the gas atoms were confined inside an ideally specularly (mirrorlike) reflecting cylinder of a 20 Å diameter.

NANOPUMPING

According to our simulation results shown in Fig. 1, the gas atoms inside the nanotube move

almost freely, along the ballistic trajectories, and they are easily accelerated to a very high axial velocity, along the direction of the traveling wave as a result of multiple synchronous collisions with the moving (traveling) nanotube walls.

Figure 1 demonstrates the nanopumping effect for 128 He atoms (black) placed inside a L=100 [Angstrom] long carbon nanotube (carbon atoms are shown by gray dots), with the diameter of 12 [Angstrom]. The nanotube has chirality of (15×0) and was built of 1,410 carbon atoms. After activating the surface traveling wave, with a frequency of 10 THz and phase velocity of 22 km/s, the helium atoms started to move in the direction of the wave propagation (in Fig.1, from left to right), from an initial 88 fs (Fig.1a), to final at 18 ps (Fig. 1d).

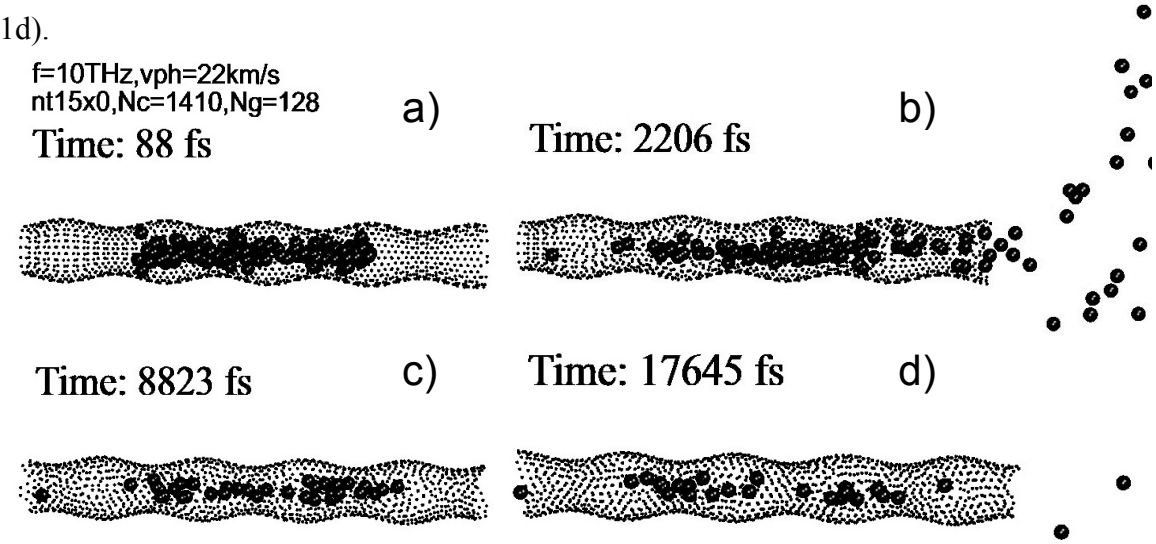

Fig. 1. Various times (from left to right) are shown from an initial 44 fs (Fig. 1a) to final at 18 ps (Fig. 1d).

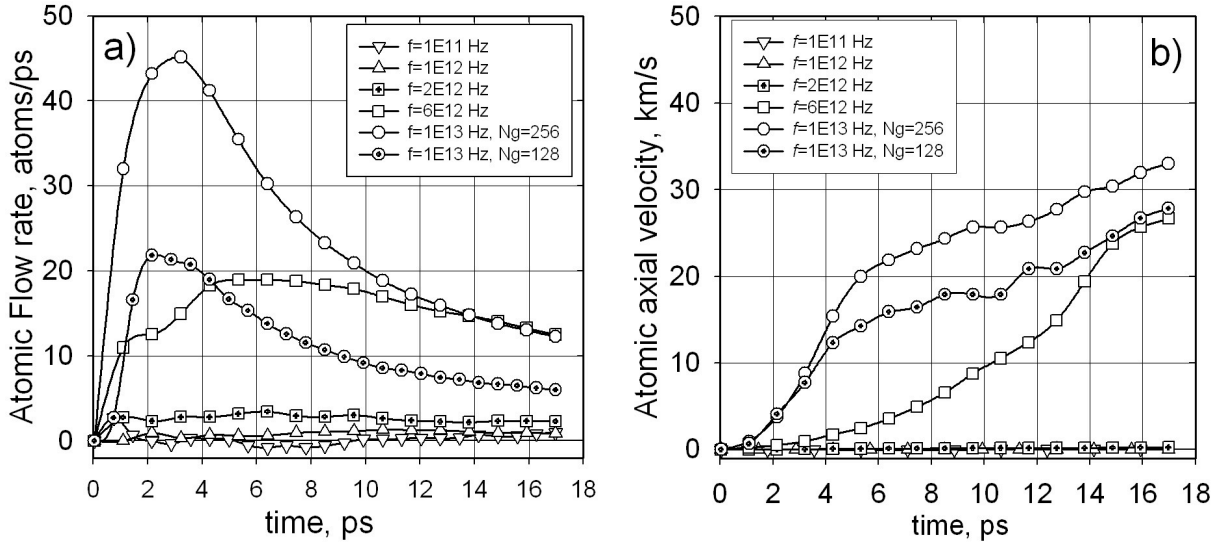

Fig. 2 (a): Dependence of flow rate through the activated nanotubes on the simulation time for various wave frequencies: 10^{11}–10^{13} Hz. (b): Average flow velocity vs. time, for various wave frequencies (1 atom/ps = 2.4×10^{-4} sccm).

Atomic fluxes generated due to the nanopumping effect for various frequencies of the surface waves for the gas initially at rest (<v>=0), are shown in Fig. 2a. The total flux increases up to a few picoseconds and then decreases as a result of the depletion of the gas inside the tube. Average axial velocities of helium atoms are given in Fig. 2b for different wave frequencies. The velocity is small below ~ 1 THz. At 6 THz the velocity reaches a hyperthermal value of ~ 30 km/s (the kinetic energy of the atoms is larger, $k_B T$).

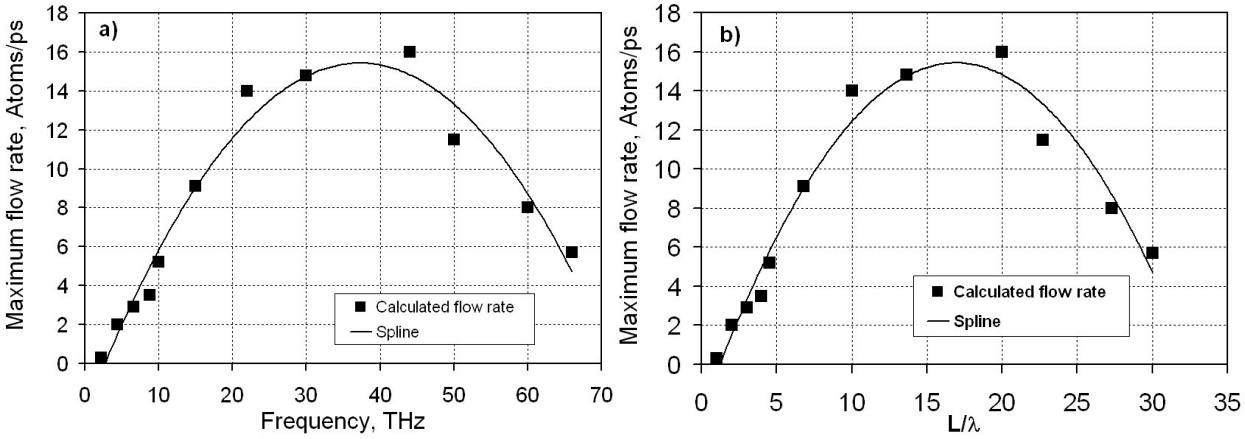

Fig. 3 (a): Dependence of the maximum flow rate on the frequency of the traveling wave; (b): Dependence of the flow rate on the ratio L/λ.

The frequency dependence of the flow rate though the nanopump is given in Fig. 3a; it will depend on the total nanotube length. Since the nanotube length was chosen to be 100 □, the characteristic frequency is high. The maximum effect is seen at approximately 38 THz. Figure 3b shows the dependence of the nanopumping effect on the ratio $L/$□, where □ the wavelength of the surface wave.

At least one physical effect closely resembles the nanopumping effect. The well-known Fermi acceleration of cosmic rays occurs when an energetic ion passes through areas with periodic magnetic fields. The Fermi acceleration is zero if the initial ion velocity is zero. Contrary to the Fermi acceleration, the nanopumping occurs in a gas at rest, with zero average velocity, for which the Fermi effect is zero.

We believe that our simulation of nanopumping through carbon nanotubes containing gas atoms and having the walls vibrated in accordance with the Rayleigh traveling wave law confirms our concept. If this hypothesis is true, the pumping effect could be used for fueling laptop computers, which is a serious engineering problem. Another example is gas pumping. Application of the new idea to the development of new turbo molecular pumps would certainly increase the pumping efficiency.

The predicted effect has similarity in nature, for example with the skin features of fast-swimming sea animals, such as dolphins. There are some indications that dolphins use specific (traveling) waves on their skin surface to damp the turbulence in the boundary layers near the skin surface. However, such mechanisms involving compliant surfaces are not yet well understood [32,33].

GAS SEPARATION BY ACTIVATED NANOTUBES

The MD simulation model of gas separation was applied to systems containing various gases with different masses. Some of the preliminary results are shown in Figs. 4-7. At the initial time, 128 gas atoms were placed inside the carbon nanotube (64 helium and 64 hydrogen atoms) (Fig. 4a). After 35 ps of generation of the Rayleigh (traveling) waves, one can see that only helium atoms are left inside the nanotube; all hydrogen atoms were pumped out in the direction of the surface waves (from left to right in Fig. 4b). We have found that the separation effect of two gases inside the nanotube is highly selective, depending strongly on the atomic mass of gases and wave frequency.

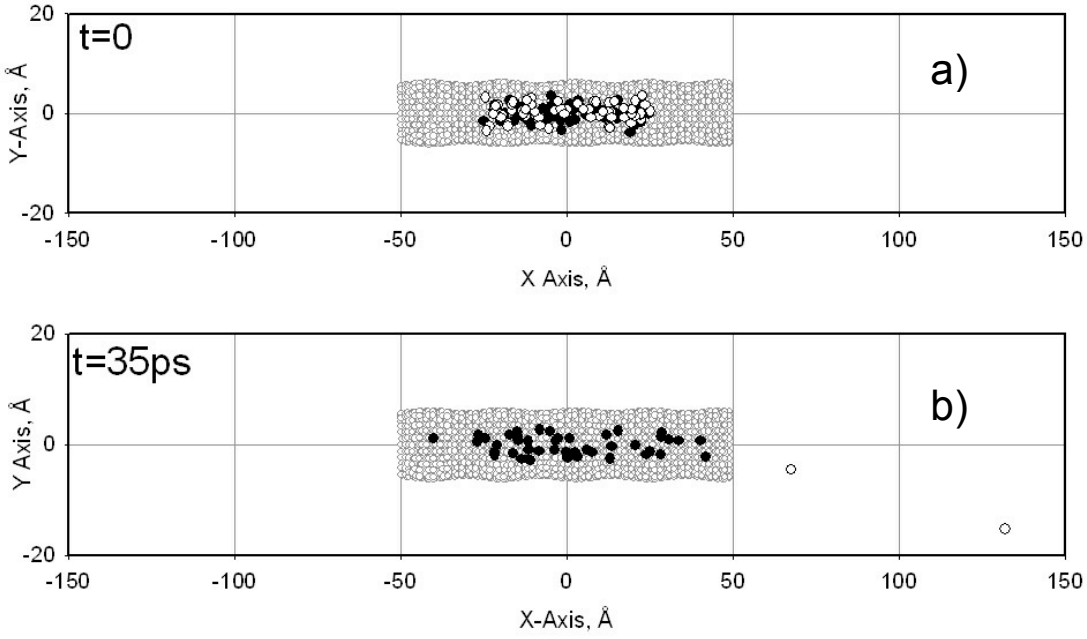

Fig. 4. The gas-separation effect strongly depends on the atomic masses of gases, wave frequency, and the phase velocity of the surface wave: (a) the initial position of 128 gas atoms inside the carbon nanotube (64 helium, and 64 hydrogen atoms); (b) position after 35 ps of generation of the Rayleigh (traveling) waves, f=10THz, on the nanotube surface: only helium atoms are left, and all hydrogen atoms are gone. (The direction of the surface wave is from left to right.)

Figure 5 shows the time dependence of the total number of helium and hydrogen atoms moved to the right side (the direction of the traveling surface wave) during the nanopumping process shown in Fig. 4. Initially, 128 gas atoms were randomly placed inside the (15×0)

carbon nanotube (64 helium and 64 hydrogen atoms). After 35 ps of generation of the Rayleigh (traveling) waves on the nanotube surface, 80% the hydrogen atoms were removed by the interaction with the walls, and only 25% of helium atoms are still left inside the nanotube. The mass-separation effect has been found even for a short nanotube length. It will be much more significant for the nanotubes of macroscopic lengths and we predict that it can be used for development of a highly selective gas sensor, a gas filter, or an isotope separation device.

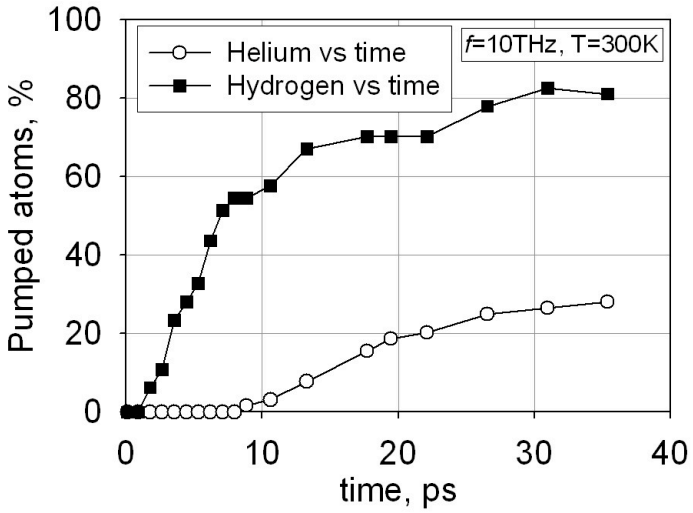

Fig. 5. The number of helium and hydrogen atoms moved from the nanotube's internal space to the right side (the direction of the traveling surface wave) during the nanopumping. 128 gas atoms were inside the {15×0} carbon nanotube (64 helium and 64 hydrogen atoms). After ~ 35 ps of generation of the waves on the nanotube surface, 80% the hydrogen atoms and 25% of helium atoms were removed by the nanopumping effect.

The gas-separation effect has also been found when the gas is placed outside the nanotube. The gas outside the nanotube was restricted inside an ideally reflecting cylinder with the radius of 20Å thus mimicking an infinite array of nanotubes. Figure 6a shows an initial position of 256 gas atoms outside the carbon nanotube (128 helium, and 128 hydrogen atoms); Figure 6b, taken after 140 ps of generation of the Rayleigh (traveling) waves, with the frequency of 10 THz and the phase velocity of 22 km/s, propagating on the nanotube surface. The final results indicating separation between hydrogen atoms that are moving to the right and helium atoms that are mostly move to the left will be given in Fig. 7.

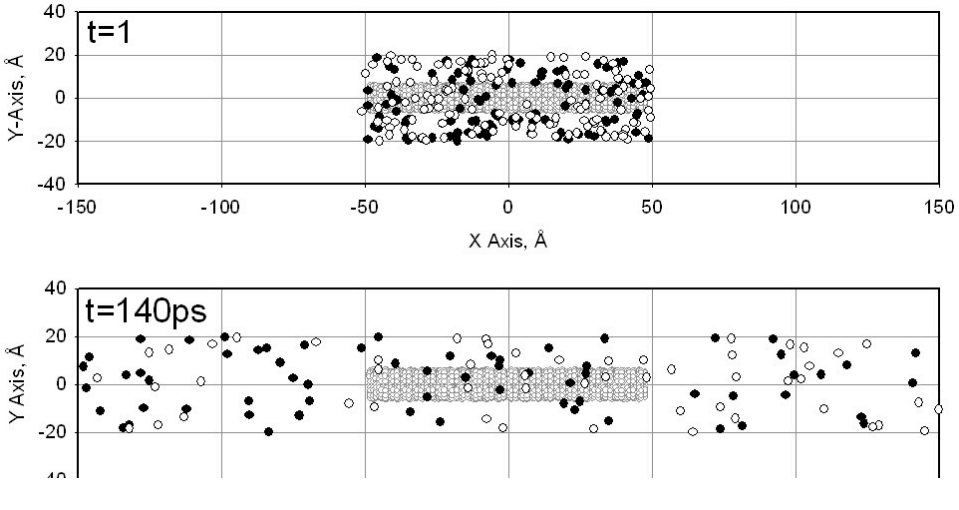

Fig. 6. Gas-separation effect for two gases placed outside the nanotube: (a) initial positions of 256 gas atoms outside the carbon nanotube (128 helium, and 128 hydrogen atoms); (b) position after 140 ps of generation of waves, f=10THz, v_{ph}= 22 km/s on the nanotube surface, showing a separation between them.

Figure 7 shows the time dependence of the gas-separation effect caused by surface traveling wave interaction with the gas outside the nanotube. The gas-separation effect seems to be less pronounced than in the case of internal gas placement in nanotube. However, it should be no difference if a large array of nanotubes (nanorope) is used since the nanotubes in the rope are vibrating with the same frequency. Figure 7 shows that hydrogen atoms are pushed to the right side (solid symbols) and helium atoms are pumped out in opposite direction (open symbols) at this frequency and wave length.

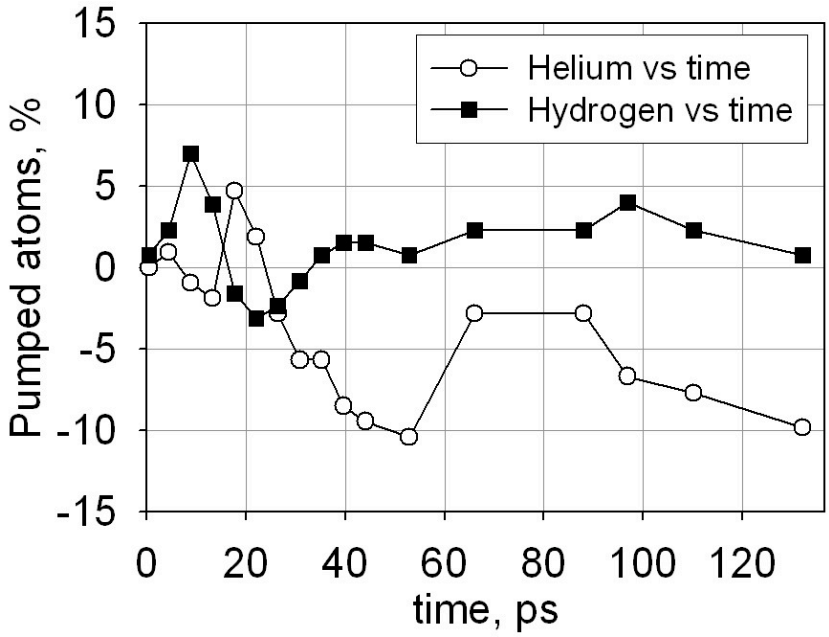

Fig. 7. A weaker gas-separation effect has been found for two gases placed outside the carbon nanotube. The solid symbols are for the hydrogen full flux in the direction of the wave (from left to right in Fig. 5). The open symbols are for helium atoms showing that helium atoms are moving backward, in opposite direction to the wave movement.

SUMMARY

We have shown that after the Rayleigh (traveling) surface waves are activated on the nanotube surface, the gas inside (or outside) of the carbon nanotube experiences multiple reflections from the nanotube walls. Depending on a combination of the atomic masses, wave frequency, phase velocity, and the relative atomic masses of the gas atoms and carbon, the gas inside the nanotube starts flowing with a macroscopic high velocity ~ 20-30 km/s, in the direction of the traveling surface wave, which we have called “nanopumping.” The driving force for both effects is the friction between the gas particles and the nanotube walls. Flow

rates and the separation rate were calculated at various frequencies and phase velocities of the surface waves. When atoms were placed outside the nanotube, one gas (hydrogen) was flowing in the direction of the Rayleigh waves, but the second gas (helium) was moving in the opposite direction. The latter effect can be used to develop a highly sensitive sensor, or a gas filter, for example for cleaning air from contamination. Such filters will be energy saving as the most energy-consuming process in the filter technology is cleaning the filter membranes. Our nanopumping effect would be able to clean the filters at a low energy consumption, by changing the direction of the surface waves.

ACKNOWLEDGMENT

This work was supported by the Office of Advanced Scientific Computing Research, Office of Science U.S. Department of Energy, under Contract DE-AC02-06CH11357.

REFERENCES

1. Darhuber, A.A., Troian, S.M. 2005, Annu. Rev. Fluid Mech. 37, 425.

2. Barrat, J.L., Bocquet L. 1999, Faraday Discuss. 112, 119.

3. Thompson, P.A., Troian, S.N. 1997, Nature (London) 389, 360.

4. Priezjev, N.V., Troian, S.M. 2004, Phys. Rev. Lett. 92, 018302.

5. Thorsen, T., Maerkl, S.J., Quake, S.R. 2002, Science 298, 580.

6. Bitsanis, I., Magda, J.J., Tirrel, M., Davis, H.T. 1987, J. Chem. Phys. 87, 1733.

7. Zengerle, R., Richter, M. 1994, J. Micromech. Microeng. 4, 192.

8. Prins, M.W.J., Welters, W.J.J., Weekamp, J.W. 2001, Science 291, 277.

9. Fan, R., Karnik, R., Yue, M., Li, D., Majumdar, A., Yang, P. 2005, Nano Lett., 5**,** 1633.

10. Kral, P., Tomanek, D. 1999, Phys. Rev. Lett. 82**,** 5373.

11. Svensson, K., Olin, H., Olsson, E. 2004, Phys. Rev. Lett., 93**,** 145901.

12. Tuzun, R.E., Noid, D.W., Sumpter, B.G., Merkle, R.C. 1996, Nanotechnology 7, 241.

13. Ni, B., Sinnot, S.B., Mikulski, P.T., Harrison, J.A. 2002, Phys. Rev. Lett. 88, 205505.

14. Supple, S., Quirke, N. 2003, Phys. Rev. Lett. 90**,** 214501.

15. Supple, S., Quirke, N. 2004, Journ. Chem. Phys. 121**,** 214501.

16. Zhang, H.W., Zhang, Z.Q., Wang, L., Zheng, Y.G., Wang, J.B., Wang, Z.K. 2007, Appl. Phys. Lett. 90, 144105.

17. Stan, G., Cole, M.W. 1998, Surf. Sci. 395, 280.

18. Simonyan, V.V., Johnson, J.K. 2002, J. Alloys and Comp., 330-332, 654.

19. Zhao, Y., Kim, Y.-H., Dillon, A.C., Heben, M.J., Zhang, S.B. 2005, Phys. Rev. Lett. 94, 155504.

20. Hirscher, M., Becher, M., Haluska, M., von Zeppelin, F., Chen, X., Dettlaff-Welikogowska, U., Roth, S. J. 2003, Alloys and Comp., 356-357**,** 433.

21. Skoulidas, A.I., Ackerman, D.M., Johnson, J.K., Sholl, D.S. 2002, Phys. Rev. Lett. 89, 185901.

22. Clausing, P. 1932, Ann. Phys. 12, 961 (English translation: 1971, J. Vac. Sci. Techn. 8, 636).

23. Sone, Y., Waniguchi, Y., Aoki, K. 1996, Phys. Fluids 8, 2227.

24. Lereu, A.L., Passian, A., Warmack, R.J., Ferrell, T.L., Thundat, T. 2004, Appl. Phys. Lett. 84, 1013.

25. Gupta, N.K., Gianchandani, Y.B. 2008, Appl. Phys. Lett. 93, 193511.

26. Clorennec, D., Royer, D. 2003, Appl. Phys. Lett. 82, 4608.

27. Natsuki, T., Hayashi, T., Endo, M. 2005, J. Appl. Phys. 97, 044307.

28. Tsukahara, Y.; Nakaso, N.; Cho, H.; Yamanaka, K. Appl. Phys. Lett. 2000, 77, 2926.
29. Clorennec, D.; Royer, D.; Walaszek, H. Ultrasonics 2002, 40, 783.
30. Telschow, K.L., Deason, V.A., Cottle, D.L., Larson III, J.D. 2000, Proc. IEEE Ultras. Symp., Puerto Rico, Oct 22-25.
31. Viktorov, I.A. 1967, Rayleigh and Lamb Waves: Physical Theory and Applications, Plenum, New York.
32. Hwang, D.P. 1997, NASA Techn. Memo. 107315, AIAA-97-0546.
33. Carpenter, P.W., Davies, C., Lucey, A.D. 2000, Current Sci. 79, 758.
34. Insepov, Z., Wolf, D., Hassanein, A. 2006, Nano Lett. 6, 1893.
35. (a) Tersoff, J. 1988, Phys. Rev. Lett. 61**,** 2879; (b) 1988, Phys. Rev. B 37**,** 6991.
36. Brenner, D. 1990, Phys. Rev. B 42, 9458.
37. Rzepka, M., Lamp, P., de la Casa-Lillo, M.A. 1998, Journ. Phys. Chem. B102, 10894.
38. Darkrim, F., Vermesse, J., Malbrunot, P., Levesque, D. 1999, Journ. Chem. Phys. 110, 4020.
39. Cheng, J., Yuan, X., Zhao, L., Huang, D., Zhao, M., Dai, L., Ding, R. 2004, Carbon 42, 2019.

Table 1. Parameters of Lennard-Jones interaction potentials for various gases and carbon

Gas	LJ radius, σ (Å)	LJ depth, ε (K)	Reference
H_2-H_2 interaction via Solvera-Goldman potential	3.41	34.3	[18]
H_2-H_2 H_2-C	2.97 3.19	33.3 30.5	[37]
H_2-H_2 H_2-C	2.958 3.179	36.7 32.05	[38]
H_2-H_2 H_2-C	2.958 3.179	36.7 32.17	[39]
He-He	2.74	16.24	[13]
He-He He-C	2.633 3.191	10.87 19.3	[7]

Supporting Online Material

Movie S1. Movie file showing a 3-D picture of the nanopumping effect for 128 helium atoms inside of a 1410 carbon atoms nanotube with chirality of (15×0), with the Rayleigh wave frequency of 10 THz, and with the phase velocity of the wave is 22 km/s. The total simulation time is 18 ps, T=300K.

Movie S2. Same simulation (S1), for the side-view showing multiple collisions of gas atoms with the nanotube walls and the pumping effect of the gas atoms inside the nanotube.

Movie S3. Movie file showing a 3-D picture of the nanopumping effect simulated for 256 helium atoms inside of a 1410 carbon atoms nanotube with chirality of (15×0), with the Rayleigh wave frequency of 10 THz, the phase velocity is 22 km/s, and the total simulation time is 18 ps, T=300K.

Movie S4. Side view of the previous simulation file (S3) showing multiple collisions of the gas atoms with the walls and the pumping effect.

Movie S5. Movie file showing a 3-D picture of the nanopumping effect simulated for 256 helium atoms inside of a 1410 carbon atoms nanotube with chirality of (15×0), with the Rayleigh wave frequency of 6 THz, the phase velocity is 22 km/s, and the total simulation time is 18 ps, T=300K.

Movie S6. Side view of the previous simulation file (S5) showing multiple collisions of the gas atoms with the walls and the pumping effect.

Movie S7. A 3-D view of the separation of a mixture of 64 helium and 64 hydrogen atoms inside a (15x0) carbon nanotube clearly showing the gas separation effect of nanopumping. A Rayleigh wave frequency of 10 THz, with a phase velocity of 22 km/s were used, the simulation time 35 ps, T=300K.

Movie S8. Side-view of the previous movie showing a gas separation effect of nanopumping.

Movie S9. Side-view of the gas separation effect where the gas is placed outside the nanotube: f=50 THz, 128 hydrogen and 128 helium atoms, T=300K, total simulation time 96 ps.